Published in final edited form as:
J Am Chem Soc. 2011 June 1; 133(21): 8062–8065. doi:10.1021/ja111613c.

^{1}H-detected ^{13}C Photo-CIDNP as a Sensitivity Enhancement Tool in Solution NMR

Jung Ho Lee[†], **Ashok Sekhar**[†], and **Silvia Cavagnero**[*,†,‡]
Biophysics Graduate Program and Department of Chemistry, University of Wisconsin, Madison, Wisconsin 53706

Abstract

NMR is a powerful yet intrinsically insensitive technique. The applicability of NMR to chemical and biological systems would be substantially extended by new approaches going beyond current signal-to-noise capabilities. Here, we exploit the large enhancements arising from ^{13}C photo-chemically induced dynamic nuclear polarization (^{13}C photo-CIDNP) in solution to improve biomolecular NMR sensitivity in the context of heteronuclear correlation spectroscopy. The ^{13}C-PRINT pulse sequence presented here involves an initial ^{13}C nuclear spin polarization via photo-CIDNP followed by conversion to antiphase coherence and transfer to ^{1}H for detection. We observe substantial enhancements, up to ≫200-fold, relative to the dark (laser off) experiment. Resonances of both side-chain and backbone CH pairs are enhanced for the three aromatic residues Trp, His and Tyr and the Trp-containing σ^{32} peptide. The sensitivity of this experiment, defined as signal-to-noise per unit time $(S/N)_t$, is unprecedented in the NMR polarization enhancement literature dealing with polypeptides in solution. Up to a 16-fold larger $(S/N)_t$ than the ^{1}H-^{13}C SE-HSQC reference sequence is achieved, for the σ^{32} peptide. This gain leads to a reduction in data collection time up to 256-fold, highlighting the advantages of ^{1}H-detected ^{13}C photo-CIDNP in solution NMR.

NMR is an invaluable spectroscopic tool to probe residue-specific molecular properties such as dynamics, folding and noncovalent interactions. To date, this technique has been largely exploited to study native and nonnative states of biomolecules in solution, including peptides, proteins and nucleic acids.[1]

Due to either scarce sample solubility,[2] the need to maintain low concentrations to overcome competing processes (e.g., aggregation), or the intrinsically low abundance of the target species in the relevant physiological environment,[3] liquid-state biomolecular NMR samples are often rather dilute, requiring highly sensitive data collection. In addition, real-time kinetic studies of fast events by NMR impose a need for rapid and efficient data collection even in concentrated samples.[4, 5]

NMR's low sensitivity stems from marginal nuclear polarization at thermal equilibrium. Enhanced polarization methods tackle this problem by perturbing the thermal equilibrium upon coupling nuclei to other highly polarized quantum states.[6] For instance, unpaired electron polarization is transferred to nuclei in dynamic nuclear polarization (DNP).[7] Parahydrogen reacts with unsaturated bonds to create ^{1}H- polarized substrates.[9] Nuclear

cavagnero@chem.wisc.edu.
[†]Biophysics Graduate Program
[‡]Department of Chemistry

Supporting Information Available: This file includes 2D ^{13}C-PRINT data on Trp, σ^{32} peptide (with no initial ^{13}C π pulse), and drkN SH3. This material is available free of charge via the Internet at http://pubs.acs.org.

polarization via coupling with rotational quantum states of methyl groups and entire small molecules leads to NMR signal enhancements by the Haupt effect[10] and hyperfine depolarization,[11] respectively. In addition, electron polarization of alkali-metals leads to hyperpolarization of noble gases via optical pumping.[12] Despite the large signal enhancements attainable by the above methods, substrates amenable to these approaches are confined to the solid-state or to small molecules in liquid solution. Promising DNP methods that polarize samples directly in the liquid state[13] or rely on the rapid thawing of prepolarized frozen solutions have proven effective for small molecules (e.g. urea, glucose)[14] and dipeptides.[15] On the other hand, the harsh rapid-dissolution procedures necessary for some of these applications are generally not desirable for large biomolecules.

A different method, photo-chemically induced dynamic nuclear polarization (photo-CIDNP) offers considerable potential and opportunities, mostly unexplored to date,[5, 16, 17, 18] as an NMR sensitivity enhancement tool for the study of both small and large biomolecules examined under mild solution conditions. According to the Radical Pair Mechanism (RPM),[19] photo-CIDNP[20, 21] proceeds via laser-triggered formation of a transient radical pair between oxidizable amino acids (typically Trp, His and Tyr) and a light-absorbing oxidizing dye (often flavin mononucleotide, FMN). After laser irradiation, the photo-excited dye in its triplet state extracts an electron from a nearby residue, giving rise to a transient radical pair. Recombination rates back to the original species depend on the hyperfine coupling between unpaired electron and the surrounding nuclei. The effect of the hyperfine coupling can be highly nuclear-spin-state-dependent, resulting in the selectively faster recombination for one of the nuclear spin states (α or β, in case of spin-1/2 nuclei). This process leads to enrichment in the fast-recombining nuclear spins, and is the key aspect of photo-CIDNP. The fraction of molecules bearing the nuclear spin state with slower recombination rate does not effectively contribute to the net polarization. In this case, the radical pairs are often sufficiently long-lived to dissociate and then undergo rapid paramagnetic nuclear relaxation, leading to thermally equilibrated spin populations at the applied field. All nuclei in solvent-exposed oxidizable residues of polypeptides and proteins are potential photo-CIDNP candidates.

The heteronuclear photo-CIDNP sensitivity enhancement efforts carried out so far focused on the Trp indole ^{15}N-^{1}H bond pair, and exploited a) ^{15}N CIDNP followed by ^{15}N→^{1}H nuclear polarization transfer,[16] b) ^{1}H CIDNP followed by ^{1}H→^{15}N→^{1}H transfer,[16, 17] c) ^{1}H→^{15}N nuclear polarization transfer followed by ^{15}N CIDNP and ^{15}N→^{1}H transfer,[18] or a combination of b) and c).[18] While these studies led to promising enhancements, their applicability is limited by the fact that the ^{15}N-^{1}H pair in the Trp indole is the only viable probe. Furthermore, the Trp indole ^{15}N-^{1}H resonances tend to be poorly dispersed in nonnative proteins.[22]

Inspired by the established existence of ^{13}C photo-CIDNP,[23, 24] the large enhancements achieved via ^{1}H-detected ^{15}N heteronuclear photo-CIDNP,[16, 18] and considering that there are many ^{13}C-^{1}H bond pairs in aromatic residues, we explored the potential of heteronuclear ^{1}H-detected ^{13}C photo-CIDNP. Here, we show that this effect leads to large NMR sensitivity enhancements in several ^{13}C-^{1}H resonances of Trp, His and Tyr, including both side chain and, intriguingly, also backbone ^{13}C$^{\alpha}$-^{1}Hs. Thus, ^{13}C photo-CIDNP followed by polarization transfer to ^{1}H enables the highly sensitive detection of both side chain and backbone resonances in amino acids, polypeptides and proteins.

As shown in Figure 1, the ^{13}C photo-CIDNP-enhanced constant time reverse INEPT (^{13}C-PRINT) pulse sequence is designed to enhance ^{13}C polarization followed by transfer to ^{1}H for detection. In the case of emissive photo-CIDNP, the initial ^{13}Cπ pulse constructively adds ^{13}C longitudinal magnetization to ^{13}C-photo-CIDNP-induced polarization. The photo-

CIDNP-inducing light beam (generated via a Spectra Physics 2017-AR in multiline mode with main lines at 488 and 514 nm, operating at 5.0 and 0.5 W for 1D and 2D experiments, respectively) was guided into the NMR sample tube inside the magnet via an optical fiber.[16, 17] Uniformly ^{13}C, ^{15}N-enriched Trp, His, Tyr, a 13-mer σ^{32} peptide (1.0 mM each) and the N-terminal SH3 domain of the drk adaptor protein from *Drosophila* (drkN SH3, 0.3 mM) were used as model substrates. All data were collected in the presence of 0.2 mM of FMN in 95%H_2O/5%D_2O adjusted to pH 7.0, at 24°C. The chemically synthesized σ^{32} peptide (see primary structure in Fig. 4) comprises the 132–144 residues of the *E. coli* σ^{32} transcriptional regulator, with Leu_{135} replaced by ^{13}C,^{15}N-Trp.[25]

Figure 2 shows that ^{13}C-^{1}H photo-CIDNP leads to significant increases in signal-to-noise per unit time $(S/N)_t$ for free Trp under laser-on (*light*) conditions, relative to both laser-off (*dark*) conditions and to a reference sensitivity-enhanced pulse-field-gradient ^{1}H-^{13}C HSQC sequence[26] in constant-time mode[27] (denoted as ^{1}H-^{13}C SE-HSQC). The observed enhancements, relative to ^{1}H-^{13}C SE-HSQC, are 12 and 4-fold for $^{13}C^{\eta 2}$-^{1}H and $^{13}C^{\alpha}$-^{1}H, respectively (Table 1). This result is particularly significant if one considers that ^{1}H-^{13}C SE-HSQC involves a full $^{1}H \rightarrow {}^{13}C \rightarrow {}^{1}H$ transfer while ^{13}C-PRINT only entails a $^{13}C \rightarrow {}^{1}H$ transfer. Even larger enhancements (41- and 22-fold) are detected, relative to dark conditions. A second type of dark experiment, denoted as dark', was also performed, with laser irradiation time (t_L) set to 0 to minimize unnecessary signal losses due to ^{13}C T_1 relaxation in the reference experiment. The observed Trp enhancements for $^{13}C^{\eta 2}$-^{1}H and $^{13}C^{\alpha}$-^{1}H relative to the dark' experiments are 27 and 14-fold, respectively (Table 1). Figure 2b shows how $(S/N)_t$ varies upon increasing t_L. After the maximum enhancement is reached, a decrease in $(S/N)_t$ at long t_L is observed under light conditions, due to reduced sample photostability and ^{13}C T_1 relaxation, both of which counteract ^{13}C photo-CIDNP buildup. This profile shows the main drawback of photo-CIDNP, i.e., the need to properly modulate laser power and irradiation time to minimize photodegradation. Comparable photo-CIDNP enhancements are also found for His and Tyr (Fig. 3, Table 1). ^{13}C,^{15}N-labeled Leu and Ser, on the other hand, experience no photo-CIDNP enhancement. Note that Tyr displays a significant C^{α} enhancement while this effect is negligible for His. Small C^{β} ^{13}C-PRINT enhancements are also observed for Trp (data not shown). These effects are smaller in steady-state than in time-resolved CIDNP[24] likely due to differences in the extent of cancellation effects.[21]

To directly address the method's applicability to larger biological systems, we analyzed the σ^{32} model polypeptide, as shown in Figure 4. Interestingly, even larger enhancements than in the case of free Trp are observed for the σ^{32} peptide. ^{13}C-PRINT yields 16-fold larger $(S/N)_t$ than ^{1}H-^{13}C SE-HSQC for C^{α}, which is 4-fold larger than the enhancement observed for free Trp (Table 1). Photo-CIDNP enhancement patterns are also different for the side chain ^{13}Cs of free Trp and the σ^{32} peptide's Trp. Specifically, a dramatic enhancement is observed for $^{13}C^{\delta 1}$ of the σ^{32} peptide Trp while a negligible effect is detected for the corresponding nucleus of free Trp (Figs 4 and S1, and Table 1). Therefore, ^{13}C photo-CIDNP enhancement patterns can be sensitive to the surrounding chemical environment.

In order to illustrate the power of ^{13}C photo-CIDNP in cases where high resolution is critical, 2D ^{13}C-PRINT data were collected for the σ^{32} peptide (Fig. 4b). Mild laser irradiation (power = 0.5W, t_L = 0.1sec) was employed in this case, to optimize sample photostability (<5% degradation) during data collection. Significant enhancements are evident here too (Fig. 4b). A comparison between Figures 4b, S1 and S2 illustrates how $(S/N)_t$ is maximized, in the case of emissive photo-CIDNP (e.g. see Trp $^{13}C^{\varepsilon 3}$, $^{13}C^{\eta 2}$), by retaining the initial ^{13}C π pulse.

Finally, we collected 2D ^{13}C-PRINT data on drkN SH3, a protein that populates both native and unfolded states in slow exchange on the NMR chemical shift timescale (Supp. Fig. S3). The greatest $(S/N)_t$ enhancements, up to 2.4-fold relative to ^{1}H-^{13}C SE-HSQC, were observed for the Trp_{36} and Tyr_{52} ^{1}H-$^{13}C^{\alpha}$ pairs in the unfolded state, Moderate enhancements (up to 1.7-fold) were also observed for the partially solvent-exposed Trp_{36} in the native state. The above experiments concisely illustrate the fact that ^{13}C-PRINT is an extremely sensitive tool to probe amino acid, peptide and protein backbone conformation.

Comparisons between ^{13}C-PRINT enhancements of amino acids, peptide and protein (Figs. 2, 4 and S3) show different relative intensities and signs. We ascribe these variations to a combination of (a) the greater extent of exchange and recombination cancellation expected for amino acids, relative to proteins, and (b) the different hyperfine constants arising from changes in electronic distribution of the different species, likely due to differences in primary structure, conformation and protonation state of the radical cation within the transient radical ion pair.[21]

In summary, this work demonstrates the power of ^{13}C photo-CIDNP in heteronuclear correlation NMR. Indeed, ^{1}H-detected ^{13}C photo-CIDNP leads to sensitivity enhancement for both side-chain and backbone CH pairs in amino acids, peptides and proteins in solution. The σ^{32} peptide sensitivity enhancement, up to 16-fold over SE-HSQC, yields a reduction in data collection time up to 256-fold and highlights the promise of this approach. $^{13}C^{\alpha}$-^{1}H enhancements are particularly noteworthy, as these nuclei are robust reporters of backbone secondary structure. While ^{13}C-PRINT is tailored to enhance resonances from specific solvent-exposed residues (Tyr, Trp and His), recent advances suggest that in the future it may be possible to transfer photo-CIDNP-enhanced C^{α} and side chain C magnetization to other nearby nuclei via NOE.[28] We anticipate that the ^{1}H-detected ^{13}C photo-CIDNP method highlighted in this work will prove useful to study of both equilibrium biological processes in dilute solutions and kinetic time-courses demanding rapid data collection.

Supplementary Material

Refer to Web version on PubMed Central for supplementary material.

Acknowledgments

We are grateful to Alexandra Yurkovskaya, Lewis Kay, Charles Fry and Milo Westler for helpful discussions, to Robert Shanks for technical assistance, and to Julie Forman-Kay for donating the drkN SH3 plasmid. This research was funded by the National Institute of Health Grant R21AI088551.

References

1. (a) Wright PE, Dyson HJ. Curr Opin Struct Biol. 2009; 19:31. [PubMed: 19157855] (b) Dyson HJ, Wright PE. Chem Rev. 2004; 104:3607. [PubMed: 15303830] (c) Gardner KH, Kay LE. Annu Rev Biophys Biomolec Struct. 1998; 27:357.(d) Farrow NA, Muhandiram R, Singer AU, Pascal SM, Kay CM, Gish G, Shoelson SE, Pawson T, Formankay JD, Kay LE. Biochemistry. 1994; 33:5984. [PubMed: 7514039]
2. (a) Kurt N, Rajagopalan S, Cavagnero S. J Mol Biol. 2006; 355:809. [PubMed: 16309705] (b) Kurt N, Cavagnero S. Biophys J. 2008; 94:L48. [PubMed: 18192369]
3. (a) Rajagopalan S, Chow C, Raghunathan V, Fry CG, Cavagnero S. J Biomol NMR. 2004; 29:505. [PubMed: 15243181] (b) Bakke CK, Jungbauer LM, Cavagnero S. Protein Expr Purif. 2006; 45:381. [PubMed: 16169747]
4. (a) Frydman L, Scherf T, Lupulescu A. Proc Natl Acad Sci U S A. 2002; 99:15858. [PubMed: 12461169] (b) Gal M, Schanda P, Brutscher B, Frydman L. J Am Chem Soc. 2007; 129:1372.

[PubMed: 17263421] (c) Giraudeau P, Shrot Y, Frydman L. J Am Chem Soc. 2009; 131:13902. [PubMed: 19743849]

5. Shapira B, Morris E, Muszkat KA, Frydman L. J Am Chem Soc. 2004; 126:11756. [PubMed: 15382886]
6. Köckenberger, W.; Matysik, J. Hyperpolarization Methods and Applications in NMR. In: John, CL., editor. Encyclopedia of Spectroscopy and Spectrometry. Elsevier; Oxford: 2010. p. 963
7. (a) Overhauser AW. Physical Review. 1953; 92:411.(b) Carver TR, Slichter CP. Physical Review. 1953; 92:212.(c) Griffin RG, et al. Phys Chem Chem Phys. 2010; 12:5725–5928.
8. Kupce E, Freeman R. J Magn Reson Ser A. 1995; 115:273.
9. Natterer J, Bargon J. Prog Nucl Magn Reson Spectrosc. 1997; 31:293.
10. Haupt J. Phys Lett A. 1972; 38:389.
11. (a) Rakitzis TP, Samartzis PC, Toomes RL, Kitsopoulos TN, Brown A, Balint-Kurti GG, Vasyutinskii OS, Beswick JA. Science. 2003; 300:1936. [PubMed: 12817146] (b) Van Brunt RJ, Zare RN. J Chem Phys. 1968; 48:4304.
12. (a) Navon G, Song Y, Room T, Appelt S, Taylor RE, Pines A. Science. 1996; 271:1848.(b) Goodson BM. J Magn Reson. 2002; 155:157. [PubMed: 12036331]
13. (a) Reese M, Turke MT, Tkach I, Parigi G, Luchinat C, Marquardsen T, Tavernier A, Hofer P, Engelke F, Griesinger C, Bennati M. J Am Chem Soc. 2009; 131:15086. [PubMed: 19803508] (b) Lingwood MD, Han SG. J Magn Reson. 2009; 201:137. [PubMed: 19783462] (c) Loening NM, Rosay M, Weis V, Griffin RG. J Am Chem Soc. 2002; 124:8808. [PubMed: 12137529]
14. (a) Ardenkjaer-Larsen JH, Fridlund B, Gram A, Hansson G, Hansson L, Lerche MH, Servin R, Thaning M, Golman K. Proc Natl Acad Sci U S A. 2003; 100:10158. [PubMed: 12930897] (b) Joo CG, Casey A, Turner CJ, Griffin RG. J Am Chem Soc. 2009; 131:12. [PubMed: 18942782]
15. Vasos PR, Comment A, Sarkar R, Ahuja P, Jannin S, Ansermet JP, Konter JA, Hautle P, van den Brandt B, Bodenhausen G. Proc Natl Acad Sci U S A. 2009; 106:18469. [PubMed: 19841270]
16. Lyon CE, Jones JA, Redfield C, Dobson CM, Hore PJ. J Am Chem Soc. 1999; 121:6505.
17. Sekhar A, Cavagnero S. J Phys Chem B. 2009; 113:8310. [PubMed: 19462951]
18. Sekhar A, Cavagnero S. J Magn Reson. 2009; 200:207. [PubMed: 19643649]
19. (a) Kaptein R, Oosterhoff JL. Chem Phys Lett. 1969; 4:195.(b) Closs GL, Closs LE. J Am Chem Soc. 1969; 91:4550.
20. (a) Bargon J, Fischer H, Johnson U. Z Naturforsch A. 1967; 22:1551.(b) Ward HR, Lawler RG. J Am Chem Soc. 1967; 89:5518.(c) Kaptein R, Dijkstra K, Nicolay K. Nature. 1978; 274:293. [PubMed: 683312] (d) Closs GL, Miller RJ, Redwine OD. Accounts Chem Res. 1985; 18:196.
21. Hore PJ, Broadhurst RW. Prog Nucl Magn Reson Spectrosc. 1993; 25:345.
22. Schlorb C, Mensch S, Richter C, Schwalbe H. J Am Chem Soc. 2006; 128:1802. [PubMed: 16464074]
23. (a) Lippmaa E, Pehk T, Buchachenko AL, Rykov SV. Chem Phys Lett. 1970; 5:521.(b) Thamarath SS, Heberle J, Hore PJ, Kottke T, Matysik J. J Am Chem Soc. 2010; 132:15542. [PubMed: 20958069]
24. Kiryutin AS, Morozova OB, Kuhn LT, Yurkovskaya AV, Hore PJ. J Phys Chem B. 2007; 111:11221. [PubMed: 17764168]
25. McCarty JS, Rudiger S, Schonfeld HJ, Schneider-Mergener J, Nakahigashi K, Yura T, Bukau B. J Mol Biol. 1996; 256:829. [PubMed: 8601834]
26. Kay LE, Keifer P, Saarinen T. J Am Chem Soc. 1992; 114:10663.
27. Cavanagh, J. Protein NMR spectroscopy: principles and practice. Academic Pr; 2007.
28. Mok KH, Kuhn LT, Goez M, Day IJ, Lin JC, Andersen NH, Hore PJ. Nature. 2007; 447:106. [PubMed: 17429353]

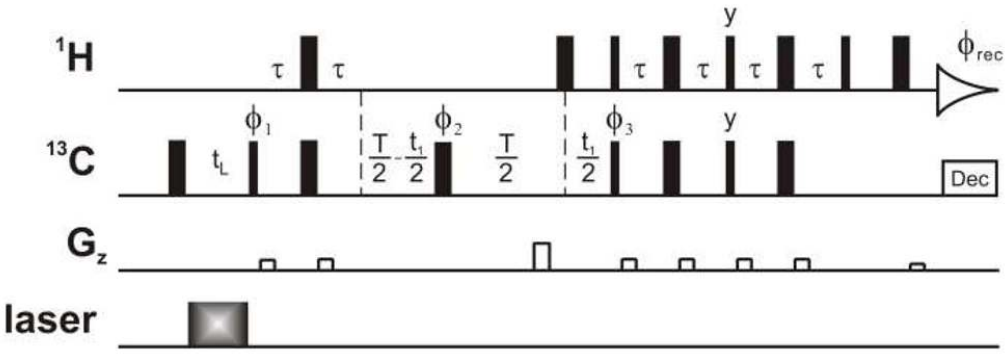

Figure 1.

^{13}C-PRINT NMR pulse sequence for ^{1}H-detected ^{13}C Photo-CIDNP-enhanced data collection. T is the total evolution time in the indirect dimension (13 and 27 ms for side chain and C^{α} carbons, respectively), for this constant-time sequence. τ is $1/4J_{CH}$ (1.6 ms) and t_L is the laser irradiation time. All pulses have x phase unless otherwise noted. ^{13}C decoupling during acquisition was performed by WURST140.[8] The phase cycling is φ_1 = y, −y; φ_2 = y, y, −x, −x, −y, −y, x, x; φ_{rec} = x, −x, −x, x. 2D experiments were run in States-TPPI mode (i.e., phase shifting of φ_1, φ_3, φ_{rec} concurrent with sign inversion of the last z-gradient). The initial ^{13}C π pulse is used to constructively add emissive ^{13}C photo-CIDNP polarization to the pre-existing ^{13}C magnetization. In the case of absorptive ^{13}C photo-CIDNP polarization, the π pulse is omitted.

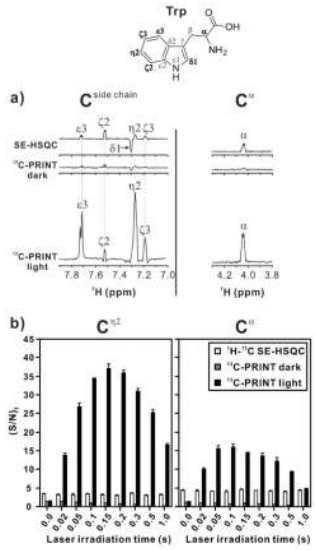

Figure 2.

a) 1D ^{13}C-PRINT NMR spectra illustrating the ^{1}H-detected ^{13}C photo-CIDNP enhancements of 1.0 mM Trp in aqueous solution. A spectral window of 6,000 Hz with 2,000 complex points was used. The t_1 carbon chemical shift evolution was set to 0. The relaxation delay was set to 1.5 s in all experiments. Four transients and two steady-state scans were collected. The data shown in this panel were acquired with a laser irradiation time t_L corresponding to the maximum $(S/N)_t$ (see t_L.dependence profiles in panel b) Spectra were phased so that resonances resulting from emissive enhancements are positive. All the NMR data shown in this work were collected on Varian INOVA 600 MHz spectrometer equipped with a triple resonance ^{1}H{^{13}C,^{15}N} triple axis gradient probe. b) Dependence of ^{13}C photo-CIDNP enhancements on the laser irradiation time t_L. Experimental conditions and acquisition parameters other than t_L are as in a). $(S/N)_t$, defined as $(S/N)/t^{1/2}$, was determined as described.[18] All measurements were carried out on 3 independent samples. Uncertainties are expressed as ±1 standard error of the mean. Note that an increase in t_L leads to a decrease in *dark* $(S/N)_t$ due to ^{13}C T_1 relaxation during laser irradiation.

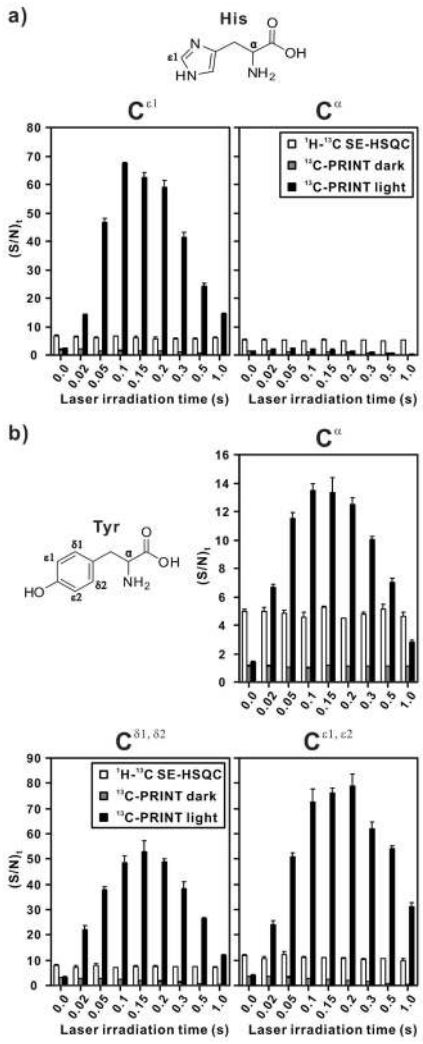

Figure 3.

Laser irradiation time dependence of photo-CIDNP enhancements of a) His and b) Tyr via ^{13}C-PRINT. Experimental parameters and error analysis are as in Figure 2. The initial ^{13}C π pulse was omitted for the data collection on Tyr C^{α} because the photo-CIDNP enhancement is absorptive, in this case.

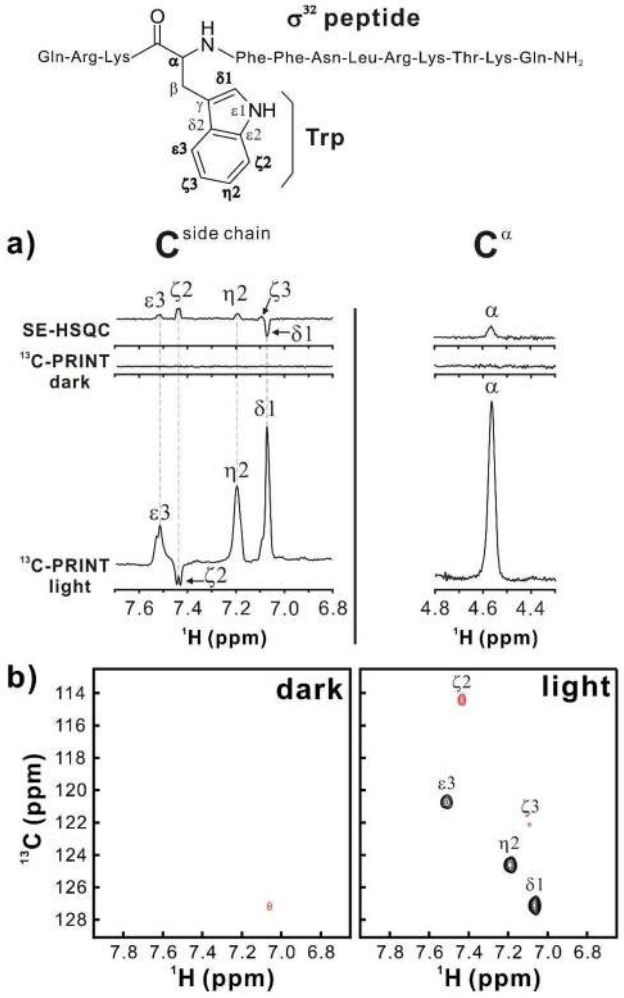

Figure 4.

a) 1D NMR spectra for the ^{1}H-detected ^{13}C photo-CIDNP enhancement of the σ^{32} peptide. Experimental procedures are as in Figure 2. b) 2D dark and light ^{13}C-PRINT spectra of the σ^{32} peptide. 2D data were collected according to States-TPPI with 32 increments per row and 1 scan per increment. Sweep widths of 6,000 Hz and 4,000 Hz were employed, for the direct and indirect dimensions, respectively. Black and red contours denote positive and negative resonances, respectively. Emissive ^{13}C photo-CIDNP enhancements originate from $C^{\delta 1}$, $C^{\varepsilon 3}$ and $C^{\eta 2}$ while absorptive enhancements are observed for $C^{\zeta 2}$ and $C^{\zeta 3}$. Note that emissive enhancements are phased to be positive.

Table 1

$(S/N)_t$ enhancements obtained via 1D ^{13}C-PRINT on Trp, His, Tyr and the σ^{32} peptide in solution.[a,b]

	Samples									
	Trp		His		Tyr			σ^{32} peptide		
Reference exp.	**η2**	**α**	**ε1**	**α**	**δ1, δ2**	**ε1 ε2**	**α**	**η2**	**δ1**	**α**
^{1}H-^{13}C SE-HSQC	11.8±0.7	3.95±0.03	10.4±0.3	0.49±0.02	6.7±0.4	7.5±0.4	2.9±0.3	12±1	6.9±0.1	16±1
^{13}C-PRINT dark	41±2	22±30	43±4	2.2±0.2	21±2	38±3	14±1	≫200[c]	≫200 [c]	220±20
^{13}C-PRINT dark'[d]	27±1	13.5±0.6	36±2	1.88±0.07	16±1	23±2	11.7±0.3	30±2	27.1±0.6	60±1

[a] The t_L value giving rise to maximums signal under light conditions (see Figure 2, 3) were used, for calculating the enhancements in this table.

[b] All uncertainties were propagated considering the ±1 standard error in $(S/N)_t$ resulting from 3 independent measurements.

[c] No explicit $(S/N)_t$ could be evaluated for these experiments because the dark spectrum lacked any detectable signal beyond the noise, even for prolonged data collection (64 transients).

[d] The notation *dark'* denotes dark reference experiments with t_L set to 0 s.

J Am Chem Soc. Author manuscript; available in PMC 2012 June 1.